Control of space-dependent four-wave mixing in a four-level atomic system

Jing Qiu,[1] Zhiping Wang,[1,*] Dongsheng Ding,[2] Zhixiang Huang,[3] and Benli Yu[1]

[1]*Key Laboratory of Opto-Electronic Information Acquisition and Manipulation, Ministry of Education, Anhui University, Hefei 230601, China*

[2]*Key Laboratory of Quantum Information, University of Science and Technology of China, Hefei, Anhui 230026, China*

[3]*Key Laboratory of Intelligent Computing and Signal Processing, Ministry of Education, Anhui University, Hefei 230039, China*

(Received 2 June 2020; revised 5 August 2020; accepted 13 August 2020; published 18 September 2020)

We propose a scheme to demonstrate the manipulation of space-dependent four-wave mixing (FWM) in a four-level atomic system. By adjusting the detuning of the control field, one can effectively control the FWM output field transferred from a pump beam carrying orbital angular momentum. More interestingly, by appropriate choice of the intensity of the control field, the FWM field can be significantly enhanced and phase twist is almost completely suppressed. Furthermore, the superposition modes created by the interference between the FWM field and a same-frequency Gaussian beam are also discussed, showing many interesting properties. Our results may open some possibilities for phase imprinting in Bose-Einstein condensates or atom manipulation with optical tweezers.

DOI: 10.1103/PhysRevA.102.033516

I. INTRODUCTION

A vortex beam carrying orbital angular momentum (OAM) [1] is nowadays an interesting resource in classical and quantum optics due to the richness of properties it shows in light-matter interactions. Unlike the conventional Gaussian beam, the OAM beam represents a fundamentally different optical degree of freedom [2] and provides unique optical properties [3], including the helical phase wavefront, which has been used in optical manipulation [4], for imaging and sensors [5], or in optical communications [6]. Due to the unique optical properties, OAM beams have also been largely used during the four-wave mixing (FWM) processes. For instance, Marino *et al.* [7] generated intensity-difference-squeezed Laguerre-Gaussian (LG) twin beams of light carrying OAM via FWM. Walker *et al.* [8] reported experimentally that the helical phase structure of OAM can be transferred from pump light to light generated in a FWM process in ^{85}Rb vapor. Quite recently, Zhang *et al.* [9] have also experimentally demonstrated the generation and propagation of a FWM vortex beam in a rubidium atomic vapor with a photonic band-gap structure. However, these scenarios do not fully manipulate the helical phase wavefront of the FWM field.

In this paper, we propose a scheme to manipulate space-dependent FWM in a four-level atomic system. The ultraslow FWM process has been an area of active research for many years [10–14], yet the FWM field is space independent and does not carry OAM. Different from those previous studies, the spatial characteristics of the FWM field carrying OAM are studied here. The major features of applying our considered scheme over other studies are as follows. First and foremost, the FWM field transferred from a pump field, which is a unique OAM mode shaped as a double-ring LG beam with the radial index $p = 1$ and the azimuthal index l, is equal but opposite in the inner ring and the outer ring. Second, by adjusting the detuning of the control field, the FWM field transferred from the pump beam can be manipulated. Third, by appropriate choice of the intensity of the control field, the FWM field can be significantly enhanced and phase twist is almost completely suppressed. It is well known that the helical phase wavefront plays a key role in the interactions of light with a medium, which will be potentially used to engineer the phase profile, for example, the phase imprinting in Bose-Einstein condensates. Moreover, we display the superposition modes created by the interference between the FWM field and a same-frequency Gaussian beam, which show a more flexible intensity control or phase control for the superposition modes. Unlike in solid-state systems [15–17], nonlinear effects are highly efficient and require only low light intensities in atomic vapors [18–20]. Therefore, this paper may be exploited for structured-beam manipulation [21–23], OAM-based quantum memory [24,25], or high-dimensional data transmission [26].

II. THEORY AND MODEL

We consider a four-level atomic system as shown in Fig. 1. States $|0\rangle$ and $|2\rangle$ are coupled by a weak Gaussian pulse field with Rabi frequency $\Omega_p = \Omega_{p0}\exp[-(x^2 + y^2)/\omega_{p0}^2]\exp(-t^2/\tau^2)$ (ω_{p0} and Ω_{p0} are the transverse waist and the initial amplitude, and τ is the pulse width), while a continuous-wave control field with Rabi frequency Ω_c drives the transition $|2\rangle \leftrightarrow |1\rangle$. The transition $|3\rangle \leftrightarrow |1\rangle$ interacts with a pump field with Rabi frequency Ω_d, and then the FWM field Ω_m is generated from the transition $|3\rangle \leftrightarrow |0\rangle$. Here, the pump field is a unique OAM mode and given as [27]

$$\Omega_d = \begin{cases} \Omega_{d0}\Omega_p^l e^{-i\phi l}, \text{ inner ring} \\ \Omega_{d0}\Omega_p^l e^{i\phi l}, \text{ outer ring} \end{cases}, \tag{1}$$

*wzping@mail.ustc.edu.cn

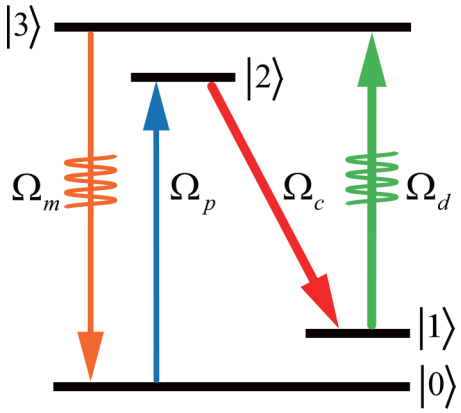

FIG. 1. Diagram of the four-level atomic system.

where $\Omega_p^l = \frac{\sqrt{2p!/\pi(p+|l|)!}}{\omega_0}(\frac{\sqrt{2}r}{\omega_0})^{|l|}L_p^{|l|}(\frac{2r^2}{\omega_0^2})e^{-r^2/\omega_0^2}$, Ω_{d0} is the initial Rabi frequency of the pump field, r is the radius, and the beam waist is ω_0. ϕ is the azimuthal angle and $L_p^{|l|}$ is the Laguerre polynomial. The radial index and azimuthal index are defined by p and l, respectively. In this paper, we set the radial index $p = 1$ while the azimuthal index l is equal but opposite in the inner ring $[0 \leqslant r \leqslant \sqrt{0.5(|l|+1)}\omega_0]$ and the outer ring $[r \geqslant \sqrt{0.5(|l|+1)}\omega_0]$.

Under the rotating-wave approximation, the terms in the Hamiltonian which oscillate rapidly are neglected. Then the Hamiltonian of the system in the interaction picture is given by

$$\begin{aligned} H_I = {} & (\Delta_p - \Delta_c)|1\rangle\langle 1| + \Delta_p|2\rangle\langle 2| + (\Delta_p - \Delta_c + \Delta_d) \\ & \times |3\rangle\langle 3| - (\Omega_p e^{i\mathbf{k}_p\cdot\hat{\mathbf{r}}}|2\rangle\langle 0| + \Omega_c e^{i\mathbf{k}_c\cdot\hat{\mathbf{r}}}|2\rangle\langle 1| \\ & + \Omega_d e^{i\mathbf{k}_d\cdot\hat{\mathbf{r}}}|3\rangle\langle 1| + \Omega_m e^{i\mathbf{k}_m\cdot\hat{\mathbf{r}}}|3\rangle\langle 0| + \text{H.c.}), \end{aligned} \tag{2}$$

where $\Delta_p = \omega_{20} - \omega_p$, $\Delta_c = \omega_{21} - \omega_c$, and $\Delta_d = \omega_{31} - \omega_d$ are the detunings of the three corresponding fields, respectively. $\mathbf{k}_j (j = p, c, d, m)$ are the wave vectors of the relevant fields. $\hat{\mathbf{r}}$ is the position vector. The symbol H.c. stands for Hermitian conjugate.

Defining the state of the atomic system as $|\psi\rangle = A_0|0\rangle + A_1 e^{i(\mathbf{k}_p-\mathbf{k}_c)\cdot\hat{\mathbf{r}}}|1\rangle + A_2 e^{i\mathbf{k}_p\cdot\hat{\mathbf{r}}}|2\rangle + A_3 e^{i(\mathbf{k}_p-\mathbf{k}_c+\mathbf{k}_d)\cdot\hat{\mathbf{r}}}|3\rangle$, the evolution equations for the probability amplitudes $A_j (j = 0, 1, 2, 3)$ can be easily obtained from the Schrödinger equation [28]:

$$\dot{A}_1 = i(\Delta_c + i\gamma_1)A_1 + i\Omega_d^* A_3 + i\Omega_c^* A_2, \tag{3a}$$

$$\dot{A}_2 = -\gamma_2 A_2 + i\Omega_c A_1 + i\Omega_p A_0, \tag{3b}$$

$$\dot{A}_3 = i(\Delta_c + i\gamma_3)A_3 + i\Omega_m A_0 + i\Omega_d A_1, \tag{3c}$$

where $\gamma_{1,2,3}$ are the corresponding decay rates of the states and the system satisfies the phase-matching condition $\mathbf{k}_m = \mathbf{k}_p - \mathbf{k}_c + \mathbf{k}_d$. Here, the pump (probe) field is assumed to be resonant with the transition.

Using the slowly varying envelope approximation, we assume that the envelope of the probe wave pulse varies slowly in time and space compared to the wavelength. So the propagation equations of the probe and FWM fields are governed by the Maxwell equation:

$$\frac{\partial\Omega_{p(m)}}{\partial z} + \frac{\partial\Omega_{p(m)}}{c\partial t} = \frac{i}{2k_{p(m)}}\nabla_\perp^2\Omega_{p(m)} + ik_{02(03)}A_{2(3)}A_0^*, \tag{4}$$

where $k_{02(03)} = 2N\omega_{p(m)}|D_{02(03)}|^2/(c\hbar)$ with N being the atomic density, and $k_{p(m)}$ is the wave number of the probe (FWM) field. $D_{02(03)}$ is the electric dipole matrix element associated with the transition from $|0\rangle$ to $|2\rangle$ ($|3\rangle$).

Assuming that the atoms are initially prepared in the ground state $|0\rangle$, Ω_c and $\Omega_d \gg \Omega_p$, and hence $|A_0|^2 \approx 1$ in the weak probe-field regime. Taking the Fourier transform of Eqs. (3) and (4), we obtain

$$(\omega + \Delta_c + i\gamma_1)\xi_1 + \Omega_d^*\xi_3 + \Omega_c^*\xi_2 = 0, \tag{5a}$$

$$(\omega + i\gamma_2)\xi_2 + \Omega_c\xi_1 + U_p = 0, \tag{5b}$$

$$(\omega + \Delta_c + i\gamma_3)\xi_3 + \Omega_d\xi_1 + U_m = 0, \tag{5c}$$

and

$$\frac{\partial U_{p(m)}}{\partial z} - \frac{i\omega}{c}U_{p(m)} = \frac{i}{2k_{p(m)}}\nabla_\perp^2 U_{p(m)} + ik_{02(03)}\xi_{2(3)}, \tag{6}$$

where the Fourier variable is defined as ω. $\xi_{i=1,2,3}$, U_p, and U_m are the Fourier transforms of $A_{i=1,2,3}$, Ω_p, and Ω_m, respectively. The first term on the right-hand side of Eq. (6) accounts for light diffraction. The diffraction term can be neglected when the Rayleigh length $\pi\omega_0^2/\lambda$ (ω_0 is the beam waist) is much larger than propagation distance L, i.e., $\pi\omega_0^2/\lambda \gg L$. In our paper, we take the propagation distance $L = 1$ cm, the transverse characteristic width $\omega_T = \omega_0 = 0.2$ mm, and the wavelength of the FWM field $\lambda = 589$ nm, obtaining $\pi\omega_T^2/\lambda \approx 21.3$ cm $\gg L$. So we neglect the diffraction term in Eq. (6).

By solving Eq. (5), one immediately obtains

$$\xi_1 = -\frac{(\omega + \Delta_c + i\gamma_3)\Omega_c^* U_p + (\omega + i\gamma_2)\Omega_d^* U_m}{M}, \tag{7a}$$

$$\xi_2 = \frac{\Omega_c\Omega_d^* U_m - M_p U_p}{M}, \tag{7b}$$

$$\xi_3 = \frac{\Omega_c^*\Omega_d U_p - M_m U_m}{M}, \tag{7c}$$

where $M = |\Omega_c|^2(\omega + \Delta_c + i\gamma_3) + |\Omega_d|^2(\omega + i\gamma_2) - (\omega + \Delta_c + i\gamma_1)(\omega + i\gamma_2)(\omega + \Delta_c + i\gamma_3)$, $M_p = |\Omega_d|^2 - (\omega + \Delta_c + i\gamma_1)(\omega + \Delta_c + i\gamma_3)$, and $M_m = |\Omega_c|^2 - (\omega + \Delta_c + i\gamma_1)(\omega + i\gamma_2)$.

Substituting Eq. (7) into Eq. (6) with the initial condition of the FWM field, $U_m(z = 0, \omega) = 0$. The analytical expressions of U_p and U_m are

$$U_p(z, \omega) = U_p(0, \omega)\frac{F_+ e^{izK_-} - F_- e^{izK_+}}{F_+ - F_-}, \tag{8a}$$

$$U_m(z, \omega) = U_p(0, \omega)\frac{F_+ F_-}{F_+ - F_-}(e^{izK_-} - e^{izK_+}), \tag{8b}$$

where $K_\pm = \omega/c + [-(k_{03}M_m + k_{02}M_p) \pm \sqrt{G}]/2M$ and $F_\pm = (k_{02}M_p - k_{03}M_m \pm \sqrt{G})/2k_{02}\Omega_c\Omega_d^*$, with $G = [k_{03}M_m - k_{02}M_p]^2 + 4k_{03}k_{02}|\Omega_c|^2|\Omega_d|^2$. In the present paper we focus on the adiabatic regime where the power series

of $K_\pm$ on ω converge rapidly. Specifically, here we take $K_\pm = K_\pm(\omega = 0) + O(\omega) + O(\omega^2)$, which is consistent with the assumption that a well-behaved adiabatic process is required for rapid conversion of a power-series expansion [29].

We can see that there exist two modes described by the dispersion relations K_+ and K_- in Eqs. (8a) and (8b). Following Ref. [30], the mode K_- will fast decay around the center frequency, which can be neglected after propagating for a longer optical depth. Then, the inverse Fourier transform of U_p and U_m can be estimated as

$$\Omega_p(z,t) = \frac{F_-}{F_- - F_+}\Omega_p(\eta_+)e^{iK_+z}, \tag{9a}$$

$$\Omega_m(z,t) = \frac{F_+F_-}{F_- - F_+}\Omega_p(\eta_+)e^{iK_+z}, \tag{9b}$$

where $\eta_+ = t - z/V_{g_+}$ and $V_{g_+} = 1/\mathrm{Re}\{[\partial K_\pm(\omega)]|_{\omega=0}\}$ is the group velocity of the K_+ mode.

Finally, the generated FWM field after a propagation distance L can be given as

$$\Omega_m(L,t) = \begin{cases} \Omega_m^l e^{-i\phi l} e^{iLK_+}, \text{ inner ring} \\ \Omega_m^l e^{i\phi l} e^{iLK_+}, \text{ outer ring} \end{cases}, \tag{10}$$

where $\Omega_m^l = k_{03}\Omega_p^l\Omega_c^*\Omega_{d0}\Omega_p(\eta_+)/\sqrt{G}$. From Eq. (10), one can find the FWM field $\Omega_m(L,t) \sim e^{\pm il\phi}$ is generated with the same vorticity as the pump field carrying OAM $\Omega_d \sim e^{\pm il\phi}$, which implies the OAM phase of field Ω_d is entirely transferred to the FWM field.

Normally, the real part $\mathrm{Re}(K_+)$ represents the variation of the phase per unit length while the imaginary part $\mathrm{Im}(K_+)$ represents the absorption [31]. Using $K_+ = \mathrm{Re}(K_+) + i\mathrm{Im}(K_+)$ we can rewrite Eq. (10) as

$$\Omega_m(L,t) = \begin{cases} \Omega_m^l e^{-L\mathrm{Im}(K_+)} e^{-i[\phi l - L\mathrm{Re}(K_+)]}, \text{ inner ring} \\ \Omega_m^l e^{-L\mathrm{Im}(K_+)} e^{i[\phi l + L\mathrm{Re}(K_+)]}, \text{ outer ring} \end{cases}, \tag{11}$$

where we can see the intensity of the FWM field in the inner and outer rings is $\propto |\Omega_m^l e^{-L\mathrm{Im}(K_+)}|^2$. The factor $e^{-i[\phi l - L\mathrm{Re}(K_+)]}$ reflects the total phase of the FWM field in the inner ring, while the factor $e^{i[\phi l + L\mathrm{Re}(K_+)]}$ reflects the total phase of the FWM field in the outer ring. Obviously, both the phase and intensity of the FWM field can be modulated via dispersion-relation term K_+.

III. DISCUSSION

Before proceeding, we briefly address the experimental feasibility of our scheme. For experimental considerations, this theoretical model can be implemented possibly for typical transitions of hyperfine-split Na D lines. For example, the lower states $|0\rangle$ and $|1\rangle$ can be assigned to $|3\,^2S_{1/2}, F = 1\rangle$ and $|3\,^2S_{1/2}, F = 2\rangle$, respectively. Two excited states $|2\rangle$ and $|3\rangle$ can be attributed to $|3\,^2P_{1/2}, F = 2\rangle$ and $|3\,^2P_{3/2}, F = 2\rangle$. The typical parameters are $\gamma_1/2\pi = 9.8 \times 10^{-4}$ MHz, $\gamma_2/2\pi = 9.8$ MHz, and $\gamma_3/2\pi = 20.42$ MHz.

In Fig. 2, we illustrate the influence of the detuning of the control field Δ_c on the phase and intensity patterns of the FWM field. As shown in Figs. 2(a) and 2(d), when the control field is tuned to the resonant interaction with the atomic transition $|2\rangle \leftrightarrow |1\rangle$, i.e., $\Delta_c = 0$, it can be seen that the phase pattern is normal and intensity distribution shows a double-ring pattern. However, when Δ_c is increased to a value $8 \times 2\pi$ MHz, the phase pattern becomes twisted, while the phase within the inner ring ($0 \leqslant r \leqslant \sqrt{2.5}\omega_0$) and the phase within the outer ring ($r > \sqrt{2.5}\omega_0$) twist oppositely [see Fig. 2(b)]. At the same time, the intensity distribution keeps unchanged but the value of intensity decreases remarkably [see Fig. 2(e)]. Interestingly, when the detuning Δ_c is adjusted to a negative value $-8 \times 2\pi$ MHz [see Figs. 2(c) and 2(f)], the intensity distribution is the same as the case in Fig. 2(e) but the rotated directions of twisted phases within two rings are completely opposite compared with the cases in Fig. 2(b). Clearly, the phase of the FWM field is modulated via the detuning of the control field.

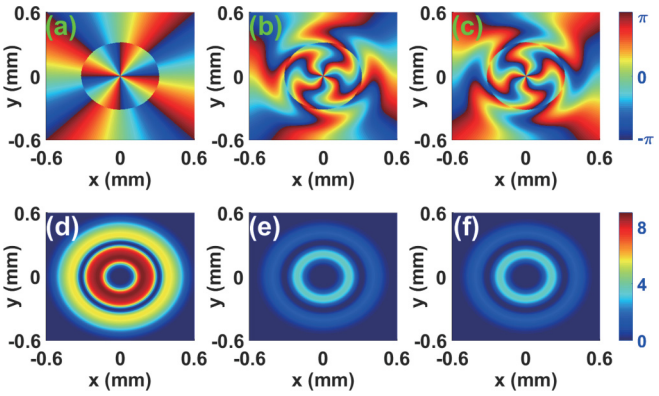

FIG. 2. (a)–(c) Phase patterns of the FWM field for different detuning of the control field Δ_c: (a) $\Delta_c/2\pi = 0$ MHz, (b) $\Delta_c/2\pi = 8$ MHz, and (c) $\Delta_c/2\pi = -8$ MHz. (d)–(f) Corresponding intensity patterns of the FWM field. The parameters are $\Omega_c/2\pi = 20$ MHz, $\Omega_{d0}/2\pi = 50$ MHz, $\omega_0 = 0.2$ mm, $\omega_{p0} = 4\omega_0$, $l = 4$, $p = 1$, $\tau = 10^{-6}$ s, $L = 1$ cm, $\Omega_{p0}/2\pi = 1$ MHz, $k_{02(03)} = 2 \times 10^9$ cm^{-1} s^{-1}.

In order to understand the above phenomena, we plot the real part and imaginary part of the dispersion relation K_+ versus radius r for different detuning Δ_c in Fig. 3. For the case $\Delta_c = 0$, as shown in Figs. 3(a) and 3(d), the value of

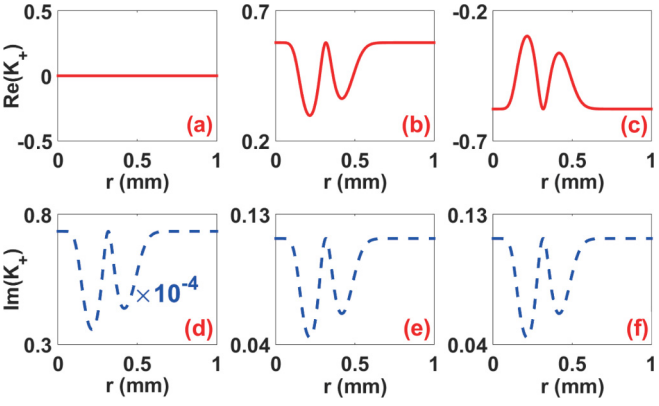

FIG. 3. The real $\mathrm{Re}(K_+)$ and imaginary $\mathrm{Im}(K_+)$ parts of the dispersion relation vs radius r for different detuning of control field Δ_c: (a), (d) $\Delta_c/2\pi = 0$ MHz, (b), (e) $\Delta_c/2\pi = 8$ MHz, and (c), (f) $\Delta_c/2\pi = -8$ MHz. Other parameters are the same as in Fig. 2.

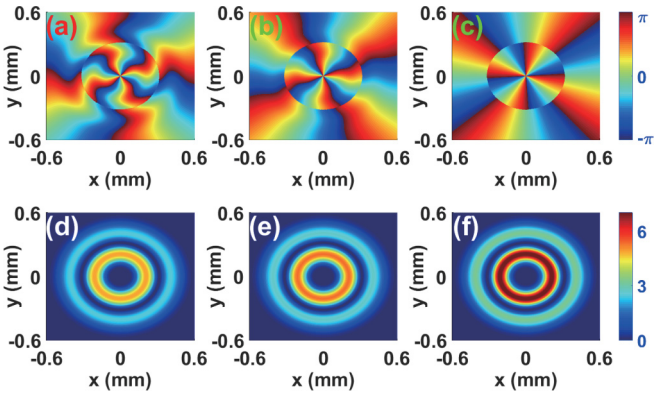

FIG. 4. (a)–(c) Phase patterns of the FWM field for different intensity of the control field Ω_c: (a) $\Omega_c/2\pi = 25$ MHz, (b) $\Omega_c/2\pi = 35$ MHz, and (c) $\Omega_c/2\pi = 45$ MHz. (d)–(f) Corresponding intensity patterns of the FWM field. Other parameters are the same as in Fig. 2(b).

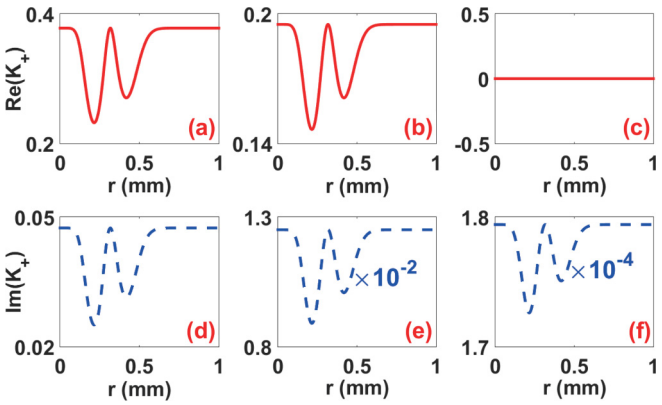

FIG. 5. The real $\mathrm{Re}(K_+)$ and imaginary $\mathrm{Im}(K_+)$ parts of the dispersion relation vs radius r for different intensity of the control field Ω_c: (a), (d) $\Omega_c/2\pi = 25$ MHz, (b), (e) $\Omega_c/2\pi = 35$ MHz, and (c), (f) $\Omega_c/2\pi = 45$ MHz. Other parameters are the same as in Fig. 2.

the imaginary part is very small ($\approx 10^{-5}$) and the real part is always equal to zero, so the phase is not twisting in Fig. 2(a). However, when $\Delta_c = \pm 8 \times 2\pi$ MHz, both the real part and imaginary part increase remarkably [see Figs. 3(b), 3(c), 3(e), and 3(f)], which means that the spatial dependencies of the phase and absorption are increasing. So one can see the phase is twisted in Figs. 2(b) and 2(c) while the value of the intensity decreases in Figs. 2(e) and 2(f). Here, note that the value of the real part in Fig. 3(b) is positive compared with the negative value of the real part in Fig. 3(c), which gives the reasonable reason that the rotated directions of the twisted phase are opposite in Figs. 2(a) and 2(c). Moreover, the imaginary part in Fig. 3(e) is the same as in Fig. 3(f), which leads to the same intensity distribution in Figs. 2(e) and 2(f).

In Fig. 4, we study the effect of the intensity of the control field Ω_c on the FWM field. From this figure, by increasing the control field, one can see that the FWM field is significantly enhanced and phase twist is almost completely suppressed in Fig. 4(c). Actually, states $|0\rangle$, $|1\rangle$, and $|2\rangle$ construct a standard electromagnetically induced transparency system [32–35]. By tuning the intensity of the control field Ω_c, the linear and nonlinear responses of the atomic medium can be easily controlled, which result in the enhancement of FWM and the suppression of phase twist. Here, it should be emphasized that the above description may provide a clue for engineering the helical phase wavefront via adjusting properly intensity of the control field, which will be potentially used to engineer the phase profile, such as phase imprinting, phase reconstructing, and phase puring. Also, we display the real and imaginary parts of the dispersion relation versus radius r for different intensity of control field Ω_c in Fig. 5. Evidently, with increasing the control field, both the real part and imaginary part are suppressed, which have readily verified the findings in Fig. 4.

Next, we further show the superposition modes created by the interference between the FWM field and a same-frequency Gaussian beam in Figs. 6 and 7. Note that the superposition intensity (or phase) pattern appears as a result of the interference between the FWM field and the Gaussian beam in a beam splitter.

Figure 6 displays the superposition modes created by the interference between the FWM field and a same-frequency Gaussian beam for different detuning of the control field Δ_c. Clearly, in the condition of $\Delta_c = 0$, it can be found from Figs. 6(a) and 6(d) that both the superposition phase and superposition intensity do not twist. When we increase Δ_c to $8 \times 2\pi$ MHz [see Figs. 6(b) and 6(e)], both superposition phase and superposition intensity become twisted, and the rotation directions of superposition patterns are opposite within the inner ring ($0 \leqslant r \leqslant \sqrt{2.5}\omega_0$) and the outer ring ($r > \sqrt{2.5}\omega_0$). Interestingly, for the case that $\Delta_c = -8 \times 2\pi$ MHz [see Figs. 6(c) and 6(f)], the twisted directions of superposition patterns are modulated and rotation directions are completely opposite compared with the situation that the value of Δ_c is positive. In such a case, the OAM mode with opposite sign of azimuthal number l shows a more flexible intensity control or phase control for the superposition mode, which may be very useful for high-dimensional light storage [36] and OAM multiplexed entanglement [37,38].

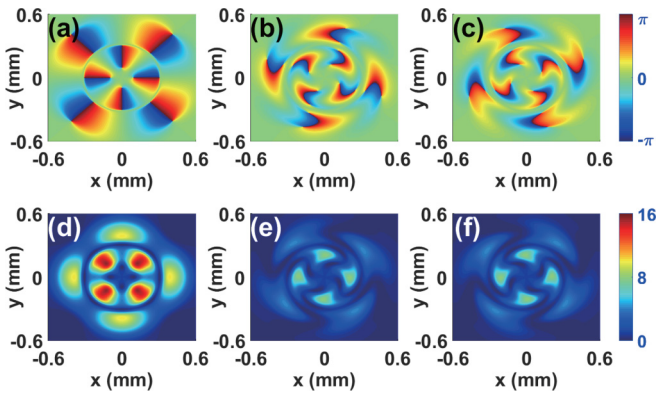

FIG. 6. (a)–(c) Superposition phase patterns created by the interference between the FWM field and a same-frequency Gaussian beam $\Omega_G = \exp(-r^2/16\omega_0^2)$ for different detuning of the control field Δ_c: (a) $\Delta_c/2\pi = 0$ MHz, (b) $\Delta_c/2\pi = 8$ MHz, and (c) $\Delta_c/2\pi = -8$ MHz. (d)–(f) Corresponding superposition intensity patterns. Other parameters are the same as in Fig. 2.

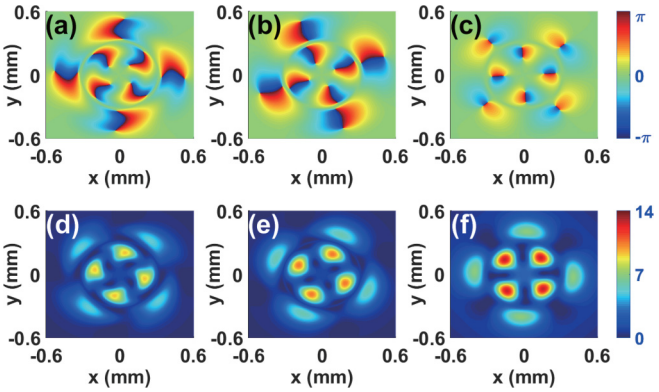

FIG. 7. (a)–(c) Superposition phase patterns created by the interference between the FWM field and a same-frequency Gaussian beam $\Omega_G = \exp(-r^2/16\omega_0^2)$ for different intensity of the control field Ω_c: (a) $\Omega_c/2\pi = 25$ MHz, (b) $\Omega_c/2\pi = 35$ MHz, and (c) $\Omega_c/2\pi = 45$ MHz. (d)–(f) Corresponding superposition intensity patterns. Other parameters are the same as in Fig. 4.

Finally, we present the superposition modes created by the interference between the FWM field and a same-frequency Gaussian beam for different intensity of the control field Ω_c in Fig. 7. As we expected, different from Fig. 6, the twists of superposition patterns are suppressed by increasing the intensity of the control field. The reason is that the intensity of the control field Ω_c modifies the azimuthal phase difference between the vortex FWM field and Gaussian beam, causing the suppression of twisted superposition patterns. In fact, the results confirm that one can effectively manipulate the OAM superposition via the intensity of the control field Ω_c.

IV. CONCLUSION

In conclusion, we propose a scheme to investigate space-dependent four-wave mixing in a four-level atomic system. Different from previous works, both the intensity and phase of the FWM field can be manipulated by adjusting the detuning of the control field. Interestingly, the enhancement of FWM and suppression of phase twist can be achieved by appropriate choice of the intensity of the control field. Moreover, we perform the superposition modes created by the interference between the FWM field and a same-frequency Gaussian reference beam. The results show that the OAM superposition modes are also manipulated via the detuning and intensity of the control field. As it is known, any light beam can be decomposed as a linear combination of the LG beams, and we can expand the pump field to the case of an arbitrary order LG mode. Thus, the method and theoretical analyses proposed here may be useful in phase imprinting of Bose-Einstein condensates [39–41], atom manipulation with optical tweezers [42], slow light [43], spatial transparency [44], structured beam generation [45], OAM energy conversion [46], vortex four-wave mixing [47–51], and quantum information science [52–56].

ACKNOWLEDGMENTS

Z.W. acknowledges financial support from the National Natural Science Foundation of China (Grant No. 11674002). D.D. acknowledges financial support from National Key Research and Development Program of China (Grant No. 2017YFA0304800) and the National Natural Science Foundation of China (Grants No. 61722510 and No. 11604322).

[1] L. Allen, M. W. Beijersbergen, R. J. C. Spreeuw, and J. P. Woerdman, Phys. Rev. A **45**, 8185 (1992).
[2] G. Molina-Terriza, J. P. Torres, and L. Torner, Nat. Phys. **3**, 305 (2007).
[3] M. Padgett, J. Courtial, and L. Allen, Phys. Today **57**(5), 35 (2004).
[4] D. G. Grier, Nature (London) **424**, 810 (2003).
[5] N. Uribe-Patarroyo, A. Fraine, D. S. Simon, O. Minaeva, and A. V. Sergienko, Phys. Rev. Lett. **110**, 043601 (2013).
[6] A. E. Willner, H. Huang, Y. Yan, Y. Ren, N. Ahmed, G. Xie, C. Bao, L. Li, Y. Cao, Z. Zhao, J. Wang, M. P. J. Lavery, M. Tur, S. Ramachandran, A. F. Molisch, N. Ashrafi, and S. Ashrafi, Adv. Opt. Photonics **7**, 66 (2015).
[7] A. M. Marino, V. Boyer, R. C. Pooser, P. D. Lett, K. Lemons, and K. M. Jones, Phys. Rev. Lett. **101**, 093602 (2008).
[8] G. Walker, A. S. Arnold, and S. Franke-Arnold, Phys. Rev. Lett. **108**, 243601 (2012).
[9] Z. Zhang, D. Ma, Y. Zhang, M. Cao, Z. Xu, and Y. Zhang, Opt. Lett. **42**, 1059 (2017).
[10] L. Deng, M. Kozuma, E. W. Hagley, and M. G. Payne, Phys. Rev. Lett. **88**, 143902 (2002).
[11] L. Deng and M. G. Payne, Phys. Rev. A **68**, 051801(R) (2003).
[12] Y. Wu, J. Saldana, and Y. Zhu, Phys. Rev. A **67**, 013811 (2003).
[13] Y. Niu, R. Li, and S. Gong, Phys. Rev. A **71**, 043819 (2005).
[14] Y. Zhang, A. W. Brown, and M. Xiao, Phys. Rev. Lett. **99**, 123603 (2007).
[15] H. H. Wang, J. Wang, Z. H. Kang, L. Wang, J. Y. Gao, Y. Chen, and X. J. Zhang, Phys. Rev. A **100**, 013822 (2019).
[16] Y. Zhang, Z. Wang, J. Qiu, Y. Hong, and B. Yu, Appl. Phys. Lett. **115**, 171905 (2019).
[17] Rahmatullah, M. Abbas, Ziauddin, and S. Qamar, Phys. Rev. A **101**, 023821 (2020).
[18] A. M. Akulshin, R. J. McLean, E. E. Mikhailov, and I. Novikova, Opt. Lett. **40**, 1109 (2015).
[19] A. Chopinaud, M. Jacquey, B. Viaris de Lesegno, and L. Pruvost, Phys. Rev. A **97**, 063806 (2018).
[20] N. Prajapati, N. Super, N. R. Lanning, J. P. Dowling, and I. Novikova, Opt. Lett. **44**, 739 (2019).
[21] A. M. Amaral, E. L. Falcão-Filho, and C. B. de Araújo, Opt. Lett. **38**, 1579 (2013).
[22] N. Radwell, T. W. Clark, B. Piccirillo, S. M. Barnett, and S. Franke-Arnold, Phys. Rev. Lett. **114**, 123603 (2015).
[23] S. Sharma and T. N. Dey, Phys. Rev. A **96**, 033811 (2017).
[24] D. S. Ding, Z. Y. Zhou, B. S. Shi, and G. C. Guo, Nat. Commun. **4**, 2527 (2013).

[25] A. Nicolas, L. Veissier, L. Giner, E. Giacobino, D. Maxein, and J. Laurat, Nat. Photonics **8**, 234 (2014).
[26] J. Wang, J. Y. Yang, I. M. Fazal, N. Ahmed, Y. Yan, H. Huang, Y. Ren, Y. Yue, S. Dolinar, and M. Tur, Nat. Photonics **6**, 488 (2012).
[27] N. Zhao, X. Li, G. Li, and J. M. Kahn, Nat. Photonics **9**, 822 (2015).
[28] M. O. Scully and M. S. Zubairy, *Quantum Optics* (Cambridge University, Cambridge, England, 1997).
[29] Y. Wu, M. G. Payne, E. W. Hagley, and L. Deng, Opt. Lett. **29**, 2294 (2004).
[30] H. J. Li and G. Huang, Phys. Rev. A **76**, 043809 (2007).
[31] Y. Wu and X. Yang, Phys. Rev. A **70**, 053818 (2004).
[32] M. Xiao, Y. Q. Li, S. Z. Jin, and J. Gea-Banacloche, Phys. Rev. Lett. **74**, 666 (1995).
[33] S. E. Harris, Phys. Today **50**(7), 36 (1997).
[34] E. Paspalakis and P. L. Knight, Phys. Rev. A **66**, 015802 (2002).
[35] M. Fleischhauer, A. Imamoglu, and J. P. Marangos, Rev. Mod. Phys. **77**, 633 (2005).
[36] D. S. Ding, W. Zhang, Z. Y. Zhou, S. Shi, G. Y. Xiang, X. S. Wang, Y. K. Jiang, B. S. Shi, and G. C. Guo, Phys. Rev. Lett. **114**, 050502 (2015).
[37] X. Pan, S. Yu, Y. Zhou, K. Zhang, K. Zhang, S. Lv, S. Li, W. Wang, and J. Jing, Phys. Rev. Lett. **123**, 070506 (2019).
[38] K. Zhang, W. Wang, S. Liu, X. Pan, J. Du, Y. Lou, S. Yu, S. Lv, N. Treps, C. Fabre, and J. Jing, Phys. Rev. Lett. **124**, 090501 (2020).
[39] Ł. Dobrek, M. Gajda, M. Lewenstein, K. Sengstock, G. Birkl, and W. Ertmer, Phys. Rev. A **60**, R3381(R) (1999).
[40] A. E. Leanhardt, A. Görlitz, A. P. Chikkatur, D. Kielpinski, Y. Shin, D. E. Pritchard, and W. Ketterle, Phys. Rev. Lett. **89**, 190403 (2002).
[41] R. Mukherjee, C. Ates, W. Li, and S. Wüster, Phys. Rev. Lett. **115**, 040401 (2015).
[42] C. Muldoon, L. Brandt, J. Dong, D. Stuart, E. Brainis, M. Himsworth, and A. Kuhn, New J. Phys. **14**, 073051 (2012).
[43] J. Ruseckas, V. Kudriašov, I. A. Yu, and G. Juzeliūnas, Phys. Rev. A **87**, 053840 (2013).
[44] X. Yang, Y. Chen, J. Wang, Z. Dou, M. Cao, D. Wei, H. Batelaan, H. Gao, and F. Li, Opt. Lett. **44**, 2911 (2019).
[45] W. Liu, R. Ma, L. Zeng, Z. Qin, and X. Su, Opt. Lett. **44**, 2053 (2019).
[46] H. R. Hamedi, E. Paspalakis, G. Žlabys, G. Juzeliūnas, and J. Ruseckas, Phys. Rev. A **100**, 023811 (2019).
[47] J. W. R. Tabosa and D. V. Petrov, Phys. Rev. Lett. **83**, 4967 (1999).
[48] H. Wang, C. Fabre, and J. Jing, Phys. Rev. A **95**, 051802(R) (2017).
[49] H.-C. Li, G.-Q. Ge, and M. S. Zubairy, Phys. Rev. A **97**, 053826 (2018).
[50] H. R. Hamedi, J. Ruseckas, and G. Juzeliūnas, Phys. Rev. A **98**, 013840 (2018).
[51] T. Jeong, J. Park, and H. S. Moon, Phys. Rev. A **100**, 033818 (2019).
[52] J. Leach, B. Jack, J. Romero, A. K. Jha, A. M. Yao, S. Franke-Arnold, D. G. Ireland, R. W. Boyd, S. M. Barnett, and M. J. Padgett, Science **329**, 662 (2010).
[53] R. Fickler, R. Lapkiewicz, W. N. Plick, M. Krenn, C. Schaeff, S. Ramelow, and A. Zeilinger, Science **338**, 640 (2012).
[54] X.-L. Wang, Y.-H. Luo, H.-L. Huang, M.-C. Chen, Z.-E. Su, C. Liu, C. Chen, W. Li, Y.-Q. Fang, X. Jiang, J. Zhang, L. Li, N.-L. Liu, C.-Y. Lu, and J.-W. Pan, Phys. Rev. Lett. **120**, 260502 (2018).
[55] Y. Wang, J. Li, S. Zhang, K. Su, Y. Zhou, K. Liao, S. Du, H. Yan, and S.-L. Zhu, Nat. Photonics **13**, 346 (2019).
[56] S. Li, X. Pan, Y. Ren, H. Liu, S. Yu, and J. Jing, Phys. Rev. Lett. **124**, 083605 (2020).